

# Edge pedestal characterisation in high triangularity Advanced Tokamak scenarios with impurity seeding at JET

*M.N.A. Beurskens<sup>1,\*</sup>, G. Arnoux<sup>2</sup>, P. de Vries<sup>1</sup>, C. Giroud<sup>1</sup>, P. Lomas<sup>1</sup>, F.G. Rimini<sup>2</sup>, A.S. Brezinsek<sup>3</sup>, C. Challis<sup>1</sup>, E. de la Luna<sup>4</sup>, W. Fundamenski<sup>1</sup>, S. Gerasimov<sup>1</sup>, E. Giovannozzi<sup>5</sup>, E. Joffrin<sup>2</sup>, A. Huber<sup>3</sup>, S. Jachmich<sup>5</sup>, X. Litaudon<sup>2</sup>, T. Loarer<sup>2</sup>, J. Mailloux<sup>1</sup>, K. McCormick<sup>7</sup>, V. Pericoli-Ridolfini<sup>5</sup>, R.A. Pitts<sup>8</sup>, R. Pugno<sup>7</sup>, E. Rachlew<sup>9</sup>, E. Solano<sup>4</sup>, M. Walsh<sup>1</sup>, L. Zabeo<sup>1</sup>, K.-D. Zastrow<sup>1</sup> and JET-EFDA Contributors<sup>#</sup>*

<sup>1</sup>EURATOM/UKAEA Fusion Association, Culham Science Centre, Abingdon, Oxon, OX14 3DB, UK<sup>1</sup>

<sup>2</sup>Association EURATOM -CEA, CEA/DSM/DRFC-Cadarache 13108, St Paul Durance, France

<sup>3</sup>Assoziationen EURATOM -Forschungszentrum, Jülich D- 52425 Jülich Germany

<sup>4</sup>Laboratorio Nacional de Fusión, Asociación EURATOM-CIEMAT, Madrid, Spain,

<sup>5</sup>Associazione EURATOM -ENEA, ENEA Centro Ricerche Frascati C.P. 65, 00044 Italy

<sup>6</sup>Association EURATOM-“Belgian State”, ERM/KMS, Brussels, Belgium, Partner in the TEC

<sup>7</sup>Association EURATOM-Max-Planck-Institut für Plasmaphysik, D-85748 Garching, Germany

<sup>8</sup>Association EURATOM, Confédération Suisse, EPFL, 1015, Lausanne, Switzerland

<sup>9</sup>Association EURATOM-VR, Department of Physics, SCI, KTH, SE-10691 Stockholm, Sweden

<sup>#</sup> Appendix of M. Watkins et al., Fusion Energy 2006 (Proc. 21st Int. Conf. Chengdu, 2006) IAEA, Vienna

## Introduction

The optimisation of performance in scenarios characterised by Internal Transport Barriers (ITB) leads, naturally, in the direction of combining the enhanced core confinement with a reduced edge transport, i.e. with an H-mode edge barrier [1,2]. The principle advantage is improved bootstrap current generation due to the edge pressure gradient: one of the best targets for JET steady-state operation is considered to be a plasma with an ITB, whose foot is located at a relatively large radius, superimposed on a strong edge pedestal. Unfortunately, this has so far proven to be an elusive goal. The cold pulse due to large periodic edge pedestal relaxations, type I ELMs, often tends to penetrate deep into the plasma and reach the foot of the ITB, causing a loss of the improved confinement inside the ITB [3,4,5,6]. In addition, plasmas with a strong edge density pedestal have reduced toroidal rotational shear, leading to a substantial decrease of the ExB shearing rate and increased difficulty in triggering and sustaining the ITB [3]. It is, therefore, important and advantageous to develop an operational regime featuring smaller ELMs, to minimise their effects on the ITB dynamics whilst maintaining as strong an edge pedestal as is compatible with the requirement of smaller ELMs

## ELM mitigation through impurity injection

The issue of ELM mitigation has recently acquired a new urgency in view of the forthcoming installation at JET of an all-metal, ITER-like wall [7,8,9]: power and energy load, both transient and steady state, to the plasma facing components will have to be reduced to ensure the survival of the metal wall.

A common technique at JET to mitigate ELMs in ITB plasmas is the injection of D2 gas or of light impurities [3,5,6]. In this paper we present results from dedicated experiments focussing on injection of both D2 and impurities and performed at JET during the 2006/2007 experimental campaigns. Two different sets of experimental scenarios have been investigated: Series 1: plasmas at relatively high current and toroidal field (3.1T /2MA) and combined heating power NBI+ICRH ~ 25 MW, the equilibrium configuration being optimized for

---

\* E-mail address of presenting author: Marc.Beurskens@jet.uk

pedestal and divertor diagnostics coverage. It is important to note that ITB triggering and optimisation of the core confinement was not a specific aim of these experiments.

Series 2: plasmas with lower current and toroidal field (2.3T/1.5MA ), aiming at achieving the maximum value of  $\beta_N$  with the available total power ( NBI + ICRH + LHCD  $\sim$  30 MW ) by producing a broad ITB combined with an H-mode edge [11].

Both experimental series had  $q_{95} \sim 5$  and high triangularity  $\delta \sim 0.45$ .

Using data from these sets of experiments, this paper will address the following questions, essential for the development of a viable scenario with both ITB and edge barrier :

- How do the pedestal and ELMs respond to extrinsic impurity seeding ?
- Is there an optimum ITB scenario with respect to ELM-characteristics (radial penetration & energy loss) that is also ITER-like wall relevant?

### Choice of Impurity

In the past, different impurities ( Neon [6], Nitrogen [10, 12], Argon [3]) have been employed at JET for ELM mitigation studies. Argon has now been abandoned because of its core accumulation and its undesirable effects on charge exchange ion temperature and rotation measurements.

In the recent experiments Neon has been used in both high and low current series, while Nitrogen has been injected only in series 1. In the case of Neon, the injection location was varied (inner & outer divertor, main chamber) and it was found that the radiative fraction achieved at a given gas rate depends on injection location. In addition, comparing Neon and Nitrogen injected at the same location, an order of magnitude more Nitrogen than Neon is required in order to obtain the same level of radiated power. The radiated fraction ( $F_{rad}$ ) in between ELMs is chosen here as parameter to quantify the strength of impurity seeding. It is defined as the ratio of the radiated power in the inter ELM period and the total input power and is a particularly useful parameter in comparing the impact on e.g. pedestal cooling of different impurity species. It is relevant given that the total input power is essentially constant throughout each of the series.

### Pedestal Parameters and ELM mitigation

In series 1 the pedestal electron temperature decreases steadily as a function of  $F_{rad}$  (fig. 1a). While the plasma remains in H-mode, this reduction is compensated by an increase in density ( Fig 1b ) so that the electron pressure remains constant . Only when a transition to L-mode occurs, the density decreases and the pressure is degraded (Fig 2a). ELM mitigation occurs in two distinct regimes at radiated fractions  $F_{rad} \sim 30\%$  and at  $F_{rad} > 50\%$  (Fig 2 b-d). In these regions high frequency ELMs occur (Fig. 2b). The diamagnetic energy loss per ELM is reduced to below 2% (Fig. 2c) and the penetration of the ELM cold pulse is limited to less than 20% of the minor radius (Fig. 2d). This sequence can possibly be explained by a transition from *low* to *high* frequency type I ELMs at  $F_{rad} \sim 30\%$  , via compound type I/III ELMs ( $F_{rad} \sim 40\%$ ) to type III ELMs ( $F_{rad} > 50\%$ ) and subsequent transition to L-mode. However, ELM identification is ongoing. Experiment series 2 (Fig 3 a-d) shows results that are consistent with those in series 1.

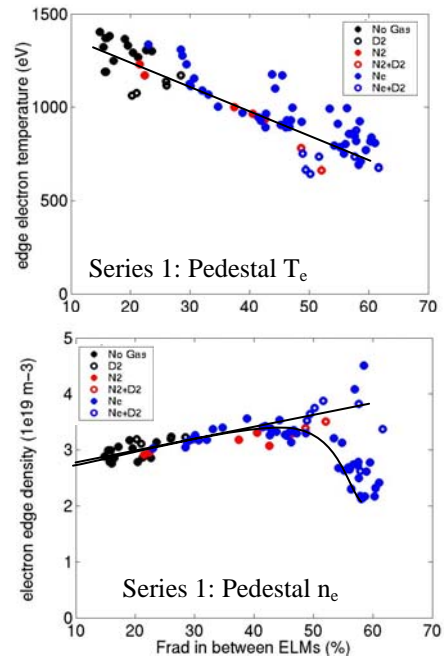


Fig. 1: pedestal  $T_e$  (ECE) and  $n_e$  (interferometry) vs  $F_{rad}$  for series 1.

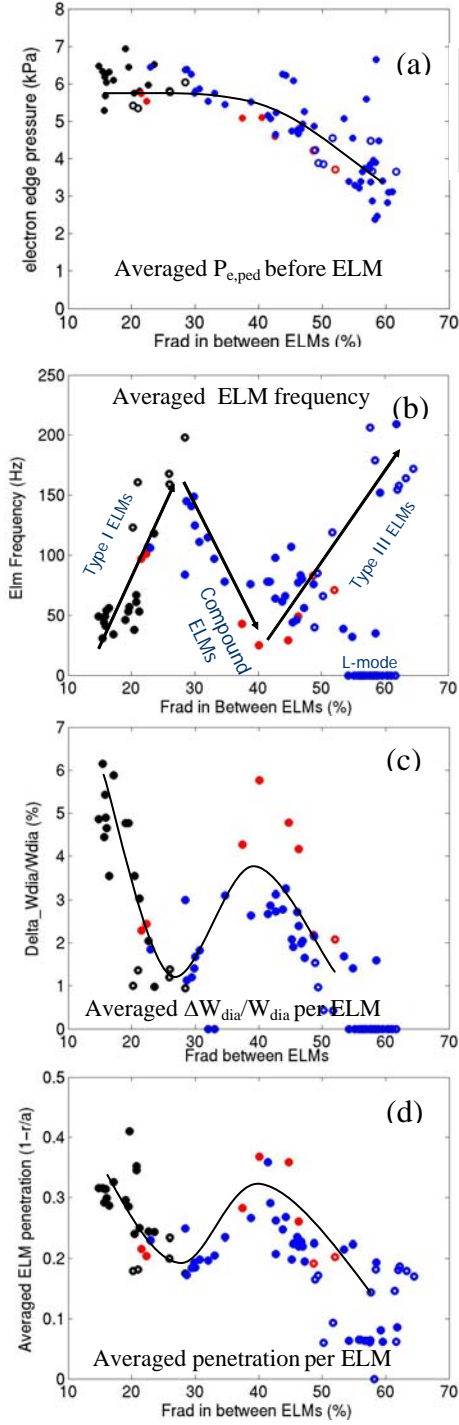


Figure 2: Series 1 (a) Electron Pedestal pressure (b) ELM Frequency (c) averaged diamagnetic energy drop per ELM (d) averaged penetration radius per ELM as a function of radiated power fraction. (ELM penetration is defined as the deepest region in the plasma where  $\Delta T_{e,ELM}/T_e > 5\%$ ) Values are time averaged over 1-2s windows.

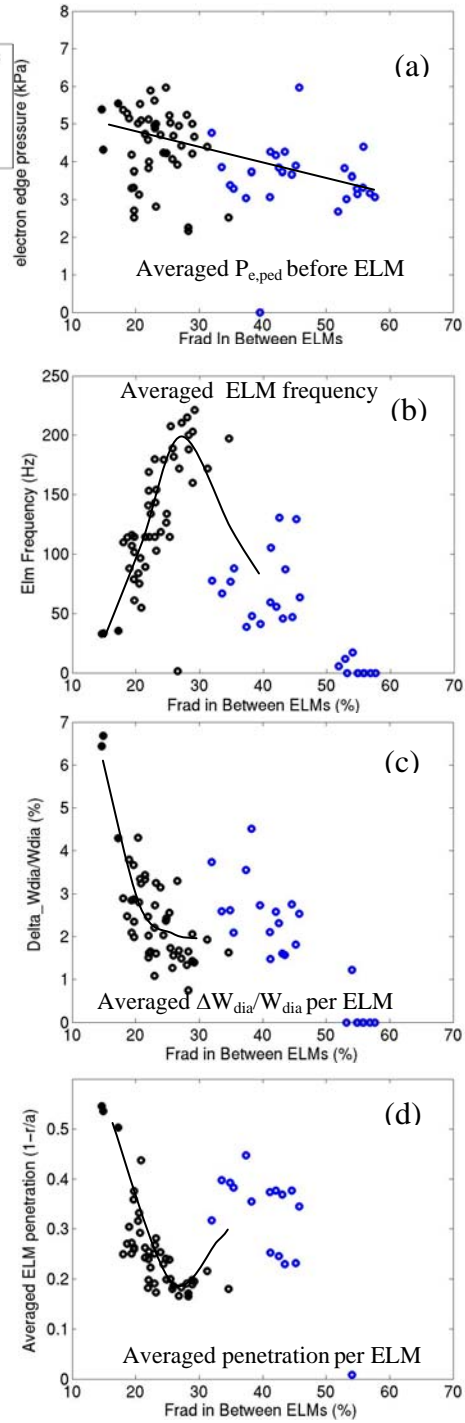


Figure 3: Series 2 (a) Electron Pedestal pressure (b) ELM Frequency (c) averaged diamagnetic energy drop per ELM (d) averaged penetration radius per ELM as a function of radiated power fraction. (ELM penetration is defined as the deepest region in the plasma where  $\Delta T_{e,ELM}/T_e > 5\%$ ) Values are time averaged over 1-2s windows.

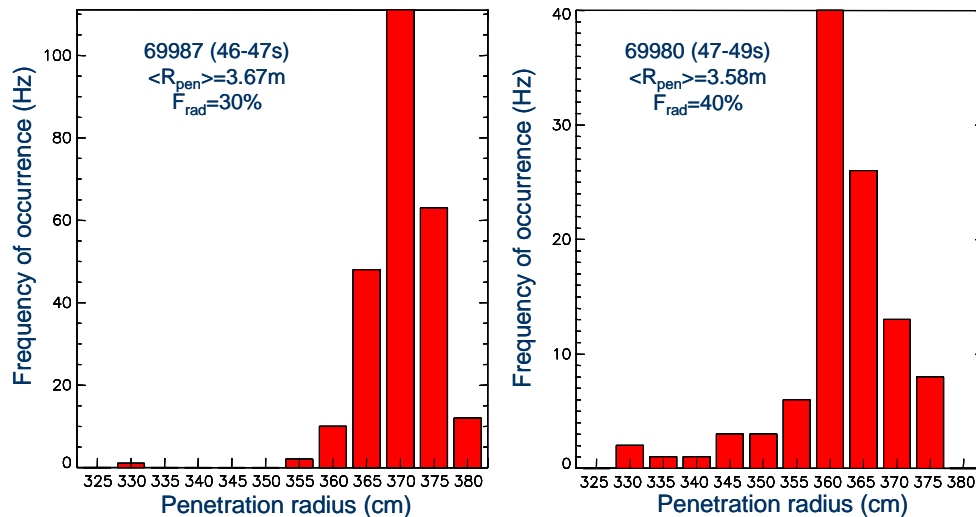


Figure 4 Histogram of Radial ELM penetration for  $F_{rad}$  of 30% and 40%

### Elm penetration statistics

Figure 3 show time averaged values for ELM energy loss,  $\Delta W_{dia}/W_{dia}$ , and ELM inwards radial penetration. It has to be stressed, however, that even a single ELM could cause the ITB to collapse if it penetrates up to its foot. Two examples of statistics of penetration radius per ELM from series 1 are given at  $F_{rad}=30\%$  and  $F_{rad}=40\%$ . (for JET:  $R_{lcfs}=3.85m$ ,  $R_0=3.1m$ ).

At  $F_{rad}=40\%$ , compound type I/III many single ELMs penetrate past half radius, where at  $F_{rad}=30\%$ , higher frequency type I, only 1 deep penetration was observed.  $\Delta W_{dia}/W_{dia}$  statistics have a similar distribution.

### Conclusions

Extrinsic impurities and D2 puffing have a beneficial impact on the pedestal in AT scenarios.  $\Delta W_{dia-ELM}/W_{dia}$  is greatly reduced to  $<2\%$ , whereas the maximum ELM penetration depth is reduced to less than 20% enhancing the possibility for the sustainment of wide ITBs. These conditions can be achieved at  $F_{rad}=30\%$  and  $F_{rad}>50\%$ . At the lower  $F_{rad}$  a good pedestal pressure is maintained, but an occasional large ELM may still occur. At  $F_{rad}>50\%$  the pedestal pressure is degraded by 30%-50%, but the ELMs are fully mitigated. The intermediate regime at  $F_{rad}\sim 40\%$  is to be avoided since large type I ELMs may occur amidst the type III phase. To achieve  $F_{rad}=30\%$  only D<sub>2</sub> fueling is required, whereas Neon seeding is needed to achieve  $F_{rad}>50\%$ . A limited number of tests have been performed with Nitrogen seeding, and the preliminary conclusion is that Nitrogen seeding does not produce better target plasmas than Neon seeding.

### References

- [1] Litaudon X. 2006 *Plasma Phys. Control. Fusion* **48** A1
- [2] Gohil P. 2002 *Plasma Phys. Control. Fusion* **44** A37
- [3] Sips A.A.C. 2001 *Nuclear Fusion*, Vol. 41, No. 11
- [4] Sarazin Y. et al 2002 *Plasma Phys. Control. Fusion* **44** 2445
- [5] Becoulet M. et al 2003 *Plasma Phys. Control. Fusion* **45** A93
- [6] Rimini F.G. et al 2005 *Nucl. Fusion* **45** 1481
- [7] Litaudon X. - this conference
- [8] Arnoux G. - this conference
- [9] Jachmich S. this conference
- [10] Monier-Garbet P. 2005 *Nucl. Fusion* **45** 1404
- [11] Mailloux J. - this conference
- [12] Corre Y. - this conference

This work was partly supported by the UK Engineering and Physical Sciences Research Council and by the European Communities under the contract of Association between EURATOM and UKAEA. The views and opinions expressed herein do not necessarily reflect those of the European Commission. This work was partly conducted under the European Fusion Development Agreement.